Anisotropic generalization of Stinchcombe's solution for the conductivity of random resistor networks on a Bethe lattice

2009 J. Phys. A: Math. Theor. 42 465001

(http://iopscience.iop.org/1751-8121/42/46/465001)

IOP PUBLISHING JOURNAL OF PHYSICS A: MATHEMATICAL AND THEORETICAL

J. Phys. A: Math. Theor. **42** (2009) 465001 (17pp) doi:10.1088/1751-8113/42/46/465001

Anisotropic generalization of Stinchcombe's solution for the conductivity of random resistor networks on a Bethe lattice

F Semeriyanov, M Saphiannikova and G Heinrich

Leibniz Institute of Polymer Research Dresden, Hohe str. 6, 01069 Dresden, Germany

E-mail: fsemeriyanov@yahoo.de

Received 16 March 2009, in final form 21 September 2009
Published 22 October 2009
Online at stacks.iop.org/JPhysA/42/465001

Abstract

Our study is based on the work of Stinchcombe (1974 *J. Phys. C: Solid State Phys.* **7** 179) and is devoted to the calculations of average conductivity of random resistor networks placed on an anisotropic Bethe lattice. The structure of the Bethe lattice is assumed to represent the normal directions of the regular lattice. We calculate the anisotropic conductivity as an expansion in powers of the inverse coordination number of the Bethe lattice. The expansion terms retained deliver an accurate approximation of the conductivity at resistor concentrations above the percolation threshold. We make a comparison of our analytical results with those of Bernasconi (1974 *Phys. Rev.* B **9** 4575) for the regular lattice.

PACS numbers: 72.80.Tm, 05.50.+q, 05.60.Cd, 05.70.Jk

1. Introduction

The random percolation theory due to Broadbent and Hammersley [1] is too simple to explain the great variety of percolation phenomena. One confronts complexity of real systems with both correlations and anisotropy playing an important role. The motivation for our study is to understand better the nature of the anisotropy in electrical conductivity of percolating systems. This is approached by means of the random resistor network (RRN) originally proposed by Kirkpatrik [2]. The resistor networks can be associated with the networks of saddle points in the conductivity profile of high-contrast systems as proved in [3]. Besides conductivity, RRN has been used to predict magnetic properties of materials [4] and even to estimate sample destruction under critical mechanical stress [5]. In the past there had been several propositions of the anisotropic percolation theories based on an assumption that the lattice bond occupation probability is *dependent* on the spatial orientations [6–10]. As a result, these theories associate the direction with the percolation threshold too, which, however, may not be true in the case of composites filled by long sticks. As found in the Monte Carlo simulations [11], the percolation threshold measured in the directions parallel and normal to the direction of the average orientation merge to a single value in the limit of infinitely large length of the sticks. Another class of anisotropic percolation theories [12, 13] assumes the occupation probability to be *independent* of the spatial directions, whereas the local conductivity is assumed to be a direction-dependent property. Unfortunately, all these theories cannot describe a peculiar phenomenon observed in geophysics. The Earth mantle exhibits the scale-dependent behavior of its conductivity anisotropy, namely its macroscopic anisotropy is much more pronounced than the microscopic one. This seems to be an indication of the fractal nature of the geological networks, see [14, 15] and references therein. The latter together with the fact that Earth drainage networks have a tree-like topology [16] makes us to believe that the topology of the resistor network behind the conductive property of the Earth mantle may also be tree-like in nature.

Using the exact Bethe lattice solution obtained by Stinchcombe [17], we propose an anisotropic RNN model that combines both the advantage of the recursive structure of a tree and the notion of a direction. In the present contribution, it will be demonstrated that the latter, being geometrically clear on a regular lattice, can be associated with the Bethe lattice as well. Unfortunately, the original paper [17] has given rise to a highly puzzling and controversial issue [13, 18] regarding the critical exponent 2 being close to the real value in 3D instead of the expected mean-field value of 3 [19]. To make the situation even more confusing, it was observed [20, 21] that Stinchcombe's solution serves as a very good approximation to the macroscopic conductivity of the resistor network on the regular 3D lattice. As highlighted by the present state of understanding of this problem [22], those two facts are just the matter of mere coincidence.

To refute this strongly negative disposition, we want to show that the correlations captured by the Bethe lattice, being controlled by the coordination number z, are sufficient to produce a very good fit to the exact solution of Bernasconi [12] for the anisotropic RNN on the regular lattice. The latter applies when the occupation probability is *well above* the critical point. At the same time, it is well known that the correlations captured are not sufficient to obtain the right critical exponents.

Technically, we generalize the Stinchcombe's calculation to the case of the anisotropic Bethe lattice, see figure 1. Besides the absence of closed loops, this structure has a special feature of being anisotropic at each node. Specifically, there are n_α bonds of α kind and n_β bonds of β kind connected at each branching point. At the same time, their total sum at a node is equal to a constant number z referred to as the coordination number of the lattice. We would like to stress that there is a large difference between the finite Bethe lattice, known also as the Cayley tree, and the infinite lattice with the surface sites neglected by definition, the difference being carefully discussed by Gujrati and Bowman [23].

The outline of the paper is as follows: in section 2, we present the model and mathematical formulation of the problem; in section 3, we present the main results; in section 4, we describe our verification of the theory with the exact solution of Bernasconi; in section 5, we describe the connection with the experiment and in section 6, we provide a discussion and conclusions. Appendices A–C provide the details of our computation.

2. Model

Unlike several previous anisotropic percolation theories [6–10] based on the model of different probabilities of filling for two types of lattice bonds, we consider the distribution of resistors to be isotropic. However, we make the local conductivities of the network elements on this special Bethe lattice to be a 'direction'-dependent, i.e. equal to σ_α and σ_β for α and β occupied bonds, respectively. The lattice itself is considered to be non-conductive. Thus, the resistors, associated with occupied bonds of the lattice, are the only conductive objects forming a tree-like network. In the mathematical form, the local conductivity distribution function is written as follows:

$$g_\alpha(\sigma) = p\delta(\sigma - \sigma_\alpha) + (1 - p)\delta(\sigma), \tag{1}$$

where p is the bond occupation probability, common for the bonds of both types. Given p and the conductivities of network elements, σ_α and σ_β, we compute the average conductivity of the network connected to a constant potential source at the origin and grounded at infinity. The question how to perform configurational averages turns out to be a difficult one.

A starting point of the present development is the observation that the percolation threshold is given by the usual equation [24]:

$$p_c = 1/(z - 1), \tag{2}$$

as its derivation does not require considerations of conductivity as such. This is the consequence of the occupation probability common for the bonds of both kinds.

Further, we define the probability distribution functions, $\phi_\alpha(b)$ and $\phi_\beta(b)$, for the average conductivity of a branch being some value b,

$$\int_0^\infty \phi_\alpha(b)\,\mathrm{d}b = 1. \tag{3}$$

Those functions measure the contribution from averaging over the ensemble sampled by resistor permutations, so that the average branch conductivity is given by

$$\overline{b_\alpha} = \int_0^\infty b\phi_\alpha(b)\,\mathrm{d}b. \tag{4}$$

Here, the symmetry $\alpha \leftrightarrow \beta$ holds for all quantities. Note that we specified in (3) and (4) the α-components, only, for the sake of brevity. The second equation is obtained readily using the $\alpha \leftrightarrow \beta$ interchange. This convention is followed everywhere in the text.

The average conductivity of a part of the tree consisting of n_α branches connected at the origin in parallel is

$$\overline{\sigma_\alpha} = n_\alpha\,\overline{b_\alpha}. \tag{5}$$

As an example, one can take $n_\alpha = n$ and $n_\beta = z - n$, which leads to $n - 1$ and $z{-}n$ of α- and β-subbranches, respectively, for the α branch (see figure 1). In order to compute $\phi_\alpha(b)$ and $\phi_\beta(b)$ we use the algorithm of [17] modified to account for the lattice anisotropic structure, detailed calculation is given in appendices A–C.

3. Results

The analytical solutions have been obtained for the two cases: (I) for the case of infinitely large coordination number, $z \to \infty$ and (II) near the percolation threshold, $p \approx p_c$. In both cases, the solution is represented in the form of a Taylor expansion in terms of the small parameters, $p_c = (z - 1)^{-1}$ and $\epsilon = (p - p_c)/p_c$, respectively.

In the first case, we obtain (see appendix B for details)

$$\overline{b_{\alpha\,(\mathrm{I})}} = -\sigma_\alpha\left(-\frac{p\sigma_\beta\Delta}{\sigma_\alpha p_c + \sigma_\beta\Delta} + \frac{\Delta}{p}\sum_{k=2}^{\infty} G^{(k)}\right), \tag{6}$$

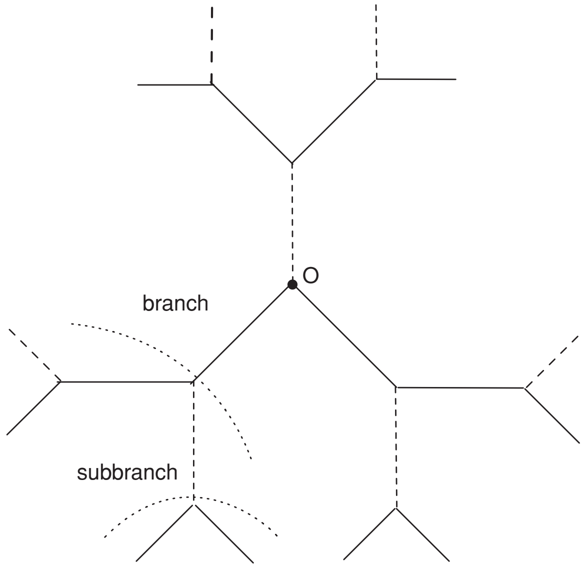

Figure 1. Anisotropic Bethe lattice of coordination number $z = 3$ with two kinds of bonds, α and β, depicted by solid and dashed lines. The center O, referred to as origin, is where n_α and n_β branches are connected by their root bonds of α and β kind, respectively. $z = n_\alpha + n_\beta$. Each branch is made of $z - 1$ subbranches connected together by their root bonds.

where

$$
\begin{aligned}
&G^{(2)} = \frac{p_c^2}{p^2}\Delta s,\\
&G^{(3)} = \frac{p_c^3}{p^5}\Delta^2 s[p(2p-1)+3\Delta s],\\
&G^{(4)} = \frac{p_c^4}{p^6}\Delta^2 s\left[3s^2\Delta - 2sp + \Delta(1-3p+3p^2) + 10\Delta^2 s\left(\frac{2p-1}{p}\right) + 15\Delta^3 s^2\frac{1}{p^2}\right],\\
&G^{(k)} = \mathrm{O}\big(p_c^k\big),\\
&\Delta = p - p_c \qquad \text{and} \qquad s = 1 - p.
\end{aligned}
\tag{7}
$$

This equation gives the average conductivity of a branch starting from the α-bond connected to a potential difference between the node at its root and the nodes at infinity. The first term is the conductivity of the infinitely branched Bethe lattice, while the summation over Gs represents the corrections up to and including the $(z-1)^{-4}$ order. To understand the differences with the isotropic case, we reproduce the expression obtained by Stinchcombe [17]:

$$\overline{b}_{\mathrm{iso(I)}} = \sigma\left(\Delta - \sum_{k=2}^{\infty} G^{(k)}\right), \tag{8}$$

with $G^{(2)}$ and $G^{(3)}$ the same as in (7), but $G^{(4)}$ being given by

$$G^{(4)} = \frac{p_c^4}{p^6}\Delta^2 s\left[3s^2\Delta - 2sp + \Delta(1-3p+3p^2) + 5\Delta^2 s\left(\frac{2p-1}{p}\right) + 15\Delta^3 s^2\frac{1}{p^2}\right]. \tag{9}$$

In the isotropic case, $\sigma_\alpha = \sigma_\beta = \sigma$, one finds that equation (8) is different from our result by the factor Δ/p before the summation. In addition, equation (9) contains the factor 5 in front of $\Delta^2 s\left(\frac{2p-1}{p}\right)$ different to 10 we have. We want point out that these discrepancies play a minor numerical role in the isotropic case as will be demonstrated in the next section.

We now calculate the critical exponents and the anisotropy near the percolation threshold, $p \approx p_c$. The details of the calculation are shown in appendix C. Close to the critical point, the integer numbers n_β and n_α are set by

$$n_\alpha \sigma_\beta = n_\beta \sigma_\alpha, \tag{10}$$

received from the symmetry considerations, equation (C.14). Qualitatively, this can be explained as follows: Bethe lattice, with its origin O representing a point inside the sample, has the branching topology of the infinite cluster. Suppose the system is just above p_c. Although the formation of the spanning cluster is a topological concept, it is qualitatively clear that the physics at p_c is dominated by singly connected bonds that are present on all length scales, which made Skal and Shklovskii [25] and de Gennes [26] to postulate that within each box of size of the correlation length ξ there is only one chain of bonds that connects its opposite edges, see also [24]. Thus, it is possible to associate the average direction of these chains with the average direction of the infinite cluster, which should be the direction where the resistance to current is minimal. For the case when the occupation probability p is the same in all directions, the direction-dependent percolation probability can only be achieved if the fraction of bonds of one kind is larger than the other. Indeed, the isotropic percolation probability $P = 1 - R^z$, where $R < 1$ is the probability of having the finite cluster [24], can be generalized to the anisotropic one, $P_\alpha = 1 - R^{n_\alpha}$, which gives $P_\alpha > P_\beta$ if $n_\alpha > n_\beta$. This leads to the following conditions:

$$n_\alpha = \frac{z\sigma_\alpha}{\sigma_\alpha + \sigma_\beta}, \qquad n_\beta = z - n_\alpha. \tag{11}$$

Thus, n_α and n_β are fixed by the local conductivities.

Returning for a moment to the previous case, we note that the Bethe lattice topology should be intact on the change of p. Thus, condition (11) has also to be applied above the critical point to obtain $\overline{\sigma_{\alpha\,(\mathrm{I})}}$ from equations (5) and (6):

$$\overline{\sigma_{\alpha\,(\mathrm{I})}} = \frac{z\sigma_\alpha}{\sigma_\alpha + \sigma_\beta}\overline{b_{\alpha\,(\mathrm{I})}}. \tag{12}$$

In the critical region, we investigate the anisotropy ratio of the network conductivities and relate this to the experimental quantity $\overline{\sigma_\parallel}/\overline{\sigma_\perp}$, where $\overline{\sigma}_{\parallel,\perp}$ are the bulk conductivities parallel and normal to the direction of an applied voltage. According to Skal and Shklovskii [25],

$$\overline{\sigma_\parallel}/\overline{\sigma_\perp} \simeq 1 + (p - p_c)^{\lambda(d)}, \tag{13}$$

where $\lambda(d)$ is a critical exponent determined by d—the dimensionality of a problem.

Straley [13], who first studied the conductivity exponent on the anisotropic Bethe lattice near the percolation threshold, obtained the anisotropy critical exponent $\lambda = 1$. Sarychev and Vinogradov [27] using the renormalization group theory and computer simulations found that $\lambda(2) = 0.9 \pm 0.1$ and $\lambda(3) = 0.3 \pm 0.1$ for 2D and 3D, respectively. Carmona and Amarti [28] deduced from experimental data for short carbon fiber reinforced polymers that $\lambda(3) \approx 0.4$. The details of our computation are given in appendix C. Our final result (C.21), written in a more concise form, is given by

$$\overline{\sigma_{\alpha\,(\mathrm{II})}} = 0.762\frac{z}{z-2}\frac{2\sigma_\alpha\sigma_\beta}{\sigma_\alpha + \sigma_\beta}\epsilon^2 + O(\epsilon^3), \tag{14}$$

where $\epsilon = (p - p_c)/p_c$. We also calculated the average anisotropy ratio near the percolation threshold (C.23):

$$\overline{\sigma_\alpha}/\overline{\sigma_\beta} = 1 + \frac{z-1}{z}\frac{\sigma_\alpha^2 - \sigma_\beta^2}{\sigma_\alpha\sigma_\beta}\epsilon + \mathrm{O}(\epsilon^2). \tag{15}$$

This result is analogous to (13) for the case when α and β are associated with the parallel and the perpendicular components, respectively. Thus, we receive the critical exponent, $\lambda = 1$, which is consistent with the exponent obtained by Straley [13] by an analogous method.

4. Comparison with the exact solution of Bernasconi

The topology of the Bethe lattice is quite different from the regular lattice, but it turns out that both models produce almost the same values of conductivity normalized to the corresponding maximum at full occupation. To achieve this correspondence, one uses the Bethe lattice with $z = 3$ and 4 and the regular lattice of 2D and 3D, respectively. To verify this we compare it with the exact solution of Bernasconi [12]. In the two-dimensional case, the exact solution on the square lattice is given by

$$x = \frac{2}{\pi} \arctan \left[\frac{x(p-x)}{a(1-x)(x+p-1)} \right]^{1/2}, \tag{16}$$

which needs to be solved for x and substituted into

$$\bar{\sigma}_{\parallel} = \sigma_{\parallel} \frac{p-x}{1-x}, \qquad \bar{\sigma}_{\perp} = \sigma_{\perp} \frac{x+p-1}{x} \tag{17}$$

to obtain the average network conductivity with the conductive elements $\sigma_{\parallel,\perp} = \sigma_{\alpha,\beta}$. In the three-dimensional case of the uniaxial symmetry, Bernasconi provides the equation

$$x = 2/\pi \arctan[2U + U^2]^{-1/2}, \tag{18}$$

with

$$U = \frac{a(1-x)(2p-1+x)}{(1+x)(p-x)}, \tag{19}$$

which needs to be solved for x and substituted into

$$\bar{\sigma}_{\parallel} = \sigma_{\parallel} \frac{p-x}{1-x}, \qquad \bar{\sigma}_{\perp} = \sigma_{\perp} \frac{2p-1+x}{1+x}. \tag{20}$$

The latter two equations can be derived in analogy with the 2D case following Bernasconi. We find that both approaches give very close predictions for a moderate anisotropy in the range of $a \simeq 0.3 \ldots 1$, see figure 2. The factor Δ/p in (6) makes the fit better, especially for the averaged component corresponding to the preferential conductivity direction. The deviations start to become significant at higher values of anisotropy, $a < 0.3$. It is clear that the discrepancy is not due to the finite number of expansion terms over $(z-1)^{-1}$, since the truncation of the summation in (6) at $k = 2$, i.e. neglecting the $k = 3, 4$ terms, preserves the good fit in the interval $[0.3 \ldots 1]$ (not shown here). Apparently, the correlations due to the loops of the regular lattice start to play more and more pronounced role upon the increase of the intrinsic anisotropy.

In view of quite good conformity of the theory for $z = 3, 4$ and the conductivity on the regular 2D and 3D lattice for moderate anisotropies, it becomes clear: (a) the fact of the fast convergence of the $(z-1)^{-1}$ expansion, because the fit becomes better as the number of expansion terms is increased and (b) the fact that the topology of the Bethe lattice, being quite different from the regular lattice, is somehow *capable to capture the correlations of the regular lattice by an adjustment of the coordination number to a lower integer value*.

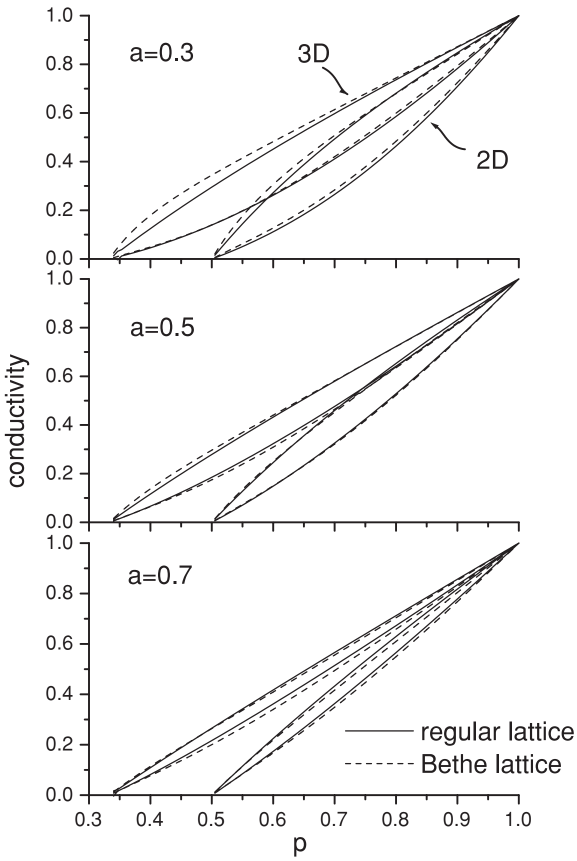

Figure 2. Comparison of $\overline{\sigma}_{(\mathrm{I})}$ given by equation (12) ($z = 3, 4$) with the exact solution of anisotropic RRN on the square and cubic lattice for three magnitudes of the local anisotropy, $a = \sigma_\perp/\sigma_\parallel = 0.3, 0.5$ and 0.7. The concave and convex curves represent macroscopic conductivity in the direction of larger and smaller local conductivity, $\sigma_\parallel$ and $\sigma_\perp$, respectively.

5. Comparison with experimental data

It is well known that the Kirkpatrick's [2] effective medium approximation (EMA), $\bar{\sigma} \sim (p - p_c)/(1 - p_c)$, is the most convenient first-order approximation widely used for experimental data far from the percolation threshold [31, 32]. Also, near the percolation threshold, the empirically observed law is $\bar{\sigma} \sim (p/p_c - 1)^t$, where t is approximately equal to 2 for 3D systems [24, 33, 34]. The Bethe lattice theory, thanks to Stinchcombe [17], readily explains the presence of both regimes: $(p - p_c)/(1 - p_c)$ and $(p/p_c - 1)^2$. It is therefore not surprising that, in the view of its elegance, the Bethe lattice has been used by us as the central paradigm of the network modeling.

The discrepancy of the critical exponent of 2 with the mean–field value of 3 suggested by de Gennes [19] is not completely clear, but can be resolved once both tree and regular lattice problem are defined in the same class of physical models. De Gennes considers the system confined by the correlation length ξ and calculates the current through the hypersurface ξ^{d-1} in d-dimensional space. On the other hand, we, who follow Stinchcombe, employ the Bethe lattice model neglecting the surface effects by definition. To make our point clear, we note that the surfaces may belong to a microscopic or macroscopic scale in general. Since the infinite branching Cayley tree cannot be embedded in a finite-dimensional space, the macroscopic surfaces in 3D are not the surface sites of the Cayley tree. On the other hand, the microscopic surfaces could, in principle, be captured by the Cayley tree, but not by the Bethe lattice where the surface sites are neglected by definition and $z = \text{const}$. Regarding the critical exponents, Bethe lattice approximation captures only weak correlations which is usually not sufficient at the critical point, but the approximation is better than the mean-field [29]. The exact mean-field limit is achieved when $z \to \infty$. Thus, in general, the Bethe lattice critical exponents are of specific nature, which implies that they may or may not coincide with the real values. An example of the coincidence can be found in the classical Flory–Stockmayer theory of sol-gel transition where the critical exponents σ and τ are found to be close to the real values of 3D [30].

6. Macroscopic versus microscopic

This section is devoted to the analysis of the paper by Straley [13]. There one finds the statement: '... the macroscopic conductivity is the average current in a link in the presence of a unit external electric field'. Let us analyze this definition carefully on the anisotropic Bethe lattice. The local current through the potential difference between two neighboring nodes is given by

$$I^n_{\alpha,\beta} = \left(V^{n-1}_{\alpha,\beta} - V^n_{\alpha,\beta}\right)\sigma_{\alpha,\beta},$$

so that the macroscopic conductivity is found from

$$\Sigma^n_{\alpha,\beta} = (Q_n - 1)\sigma_{\alpha,\beta},$$

where

$$\Sigma^n_{\alpha,\beta} = \frac{I^n_{\alpha,\beta}}{V^n_{\alpha,\beta}} \qquad \text{and} \qquad Q_n = \frac{V^{n-1}_\alpha}{V^n_\alpha} = \frac{V^{n-1}_\beta}{V^n_\beta}.$$

The fact that Q_n is independent of α and β follows from the occupation probability p being independent of those indices. For simplicity, we show the proof only for the case of fully occupied, $p = 1$, Bethe lattice. With the help of Kirchoff's law which states that the sum of the currents on each internal site is zero,

$$V_i = \frac{\sum_j \sigma_{ij} V_j}{\sum_{ij} \sigma_{ij}},$$

the formulation of the problem in terms of the recurrent relations is straightforward. For instance, for the case of coordination number $z = 4$ we have the following recursive relations:

$$V^n_\alpha = \frac{V^{n+1}_\alpha \sigma_\alpha + 2V^{n+1}_\beta \sigma_\beta + V^{n-1}_\alpha \sigma_\alpha}{2\sigma_\alpha + 2\sigma_\beta},$$

$$V^n_\beta = \frac{V^{n+1}_\beta \sigma_\beta + 2V^{n+1}_\alpha \sigma_\alpha + V^{n-1}_\beta \sigma_\beta}{2\sigma_\alpha + 2\sigma_\beta}.$$

Dividing both sides of the equations by V^{n-1}_α and V^{n-1}_β, respectively, gives the recursive relations for the ratios $Q^n_{\alpha,\beta} = V^{n+1}_{\alpha,\beta}\big/V^n_{\alpha,\beta}$ and $Y^n_{\alpha,\beta} = V^{n+1}_{\alpha,\beta}\big/V^n_{\beta,\alpha}$. Performing the iterations from an arbitrary initial values of the ratios, one finds $Q^n_{\alpha,\beta}$ being independent of α and β, $Q^n_{\alpha,\beta} = Q_n$. In the limit of very large number of iterations, one arrives to the fixed point $Q_n \to Q$ with the conductivity expressed as

$$\Sigma_{\alpha,\beta} = (Q - 1)\sigma_{\alpha,\beta},$$

which tells us that the ratio of the conductivities in two directions is just the ratio of the conductive elements:

$$\Sigma_\alpha/\Sigma_\beta = \sigma_\alpha/\sigma_\beta.$$

Here, the factor $Q - 1$ measures the average ratio of potentials of two neighboring nodes which gives the average current in a link. We note that this is the maximum value anisotropy as a function of p assuming that the resistors are distributed homogeneously. While this relationship is the correct one for the regular lattice, this model fails to explain considerably higher values of macroscopic anisotropy of the Earth mantle as compared to the microscopic ones. Presuming that the distribution of conductive inclusions is homogeneous, only a fractal structure could possibly explain this experimental observation. Thus, the definition of the macroscopic conductivity on the Bethe lattice proposed by Straley seems to be incapable of accounting for the anisotropy growth upon the change from the microscopic to the macroscopic scale.

7. Discussion and conclusions

We propose the model of the resistor network that has a property of anisotropy in a sense that the conductivities of the resistors differ with respect to the lattice bond type. We solve the problem in the framework of the anisotropic Bethe lattice approximation. The mathematical problem is formulated in terms of a nonlinear integral equation, which is solved asymptotically using series expansions in two limiting cases: near the percolation threshold and near the mean-field limit of $z \to \infty$.

It seems that the Bethe lattice may be a suitable model for the conductivity anisotropy of geological resistor networks far from the percolation threshold. Generally speaking, a Bethe lattice branch, see figure 1, is one of many possible models of a statistically homogeneous random graph. By homogeneity we mean allowing for only very small fluctuations of coordination numbers of the nodes. For the purpose of the large-scale characterization of the network, the coordination numbers of different nodes (vertices) can be approximately considered as uniform and equal to an average value. One possibility is to use the wholly tree-like structure in which the average shortest path length scales as a power of the total number of vertices [35]. Another possibility would be to use the model of small-world network where the average shortest path is signified by the logarithmic dependence on the graph size [36]. These are two theoretical examples of the different specific classes of real-world networks empirically observed. The significant anisotropies observed in geophysics at the macroscale could be explained by the formation of fractal structures in a microscale. In the present model, the macroscopic observable anisotropy is the property of the entire network and the local (intrinsic) anisotropy is associated with the anisotropy in conductivity at a branching point of the Bethe lattice. The former is defined as $\overline{a} = \overline{\sigma_\beta}/\overline{\sigma_\alpha}$, whereas the latter is essentially the ratio $a = \sigma_\beta/\sigma_\alpha$ being the *only* parameter entering equations (6), (7) and (12). We find that the present theory is capable of producing the strong global anisotropy, $\overline{a}$, at small local anisotropy, a, in the case when z is large and $p \gg p_c$. Indeed, in this limit, the conductivity is given by the mean-field formula: $\overline{\sigma_\alpha}_{(\mathrm{I})} \approx zp\sigma_\alpha^2\big/(\sigma_\alpha + \sigma_\beta)$, which yields $\overline{a}_{(\mathrm{I})} \approx a^2$. In many cases, the dynamical networks are driven to criticality, but the networks driven far away from the critical point are also realizable in principle and possible to occur in nature. Interestingly, the previous theories based on anisotropic occupation probability [7, 10] predicted the opposite: at strong local anisotropy—weak global one.

In the course of our derivation, we employed the approximation that the number of the special directions n remains finite as $z \to \infty$. Although it is not possible to give a simple geometrical picture relating n to some normal space coordinates, since Bethe lattice cannot be embedded in a finite-dimensional space, the number n seems to be associated with the the number of possible directions of the spanning cluster near the percolation threshold. The problem needs to be resolved on more rigorous topological grounds.

Acknowledgments

FS is grateful to Professor P D Gujrati for many fruitful discussions and kind attention. We also thank the anonymous referees for their valuable comments and constructive criticism. The financial support of the German Federal Ministry of Education and Research (BMBF) under the project CarboNet no 03X0504E is gratefully acknowledged.

Appendix A. Anisotropic Bethe lattice theory

This section is essentially the anisotropic generalization of [17] with the intermediate steps shown explicitly in [37]. For a branch starting from an α-bond and its $z-1$ next-generation subbranches (see figure 1), the set of conductivities is defined:

$$\left\{b_\alpha^{(i)}\right\} = b_\alpha^{(0)}, b_\alpha^{(1)}, \ldots, b_\alpha^{(n_\alpha-1)}, b_\beta^{(n_\alpha)}, \ldots, b_\beta^{(z-1)},$$

which are zero or finite accordingly as the corresponding root bonds are empty or occupied, where the index $i = 0$ is reserved for the branch origin. These subbranches are connected in parallel, so that the conductivities $b_\alpha^{(0)}$ are given by

$$b_\alpha^{(0)} = \sum_{i=1}^{n_\alpha-1} \frac{\sigma_\alpha b_\alpha^{(i)}}{\sigma_\alpha + b_\alpha^{(i)}} + \sum_{i=n_\alpha}^{z-1} \frac{\sigma_\beta b_\beta^{(i)}}{\sigma_\beta + b_\beta^{(i)}}. \tag{A.1}$$

Both $b_\alpha^{(i)}$ $\left(b_\beta^{(i)}\right)$ and σ_α (σ_β), which are the branch and bond conductivities, respectively, are random variables distributed with some probability density functions. In order to determine the branch distribution functions $\phi_\alpha(b^{(0)})$ defined in (3) and (4), we average over various resistor configurations on the lattice using the distribution functions $\phi_\alpha(b^{(i)})$ and $g_\alpha(\sigma^{(i)})$ defined for the conductivities of subbranches and individual bonds, respectively, so that

$$g_\alpha(\sigma) = p\,\delta(\sigma - \sigma_\alpha) + (1-p)\delta(\sigma). \tag{A.2}$$

Being more specific we determine $\phi_\alpha(b)$ (note that the superscript (0) is suppressed for brevity) by performing an asymptotic analysis of

$$\phi_\alpha(b) = \prod_{i=1}^{n_\alpha-1} \left(\int_0^\infty \mathrm{d}\sigma^{(i)}\, g_\alpha(\sigma^{(i)}) \int_0^\infty \mathrm{d}b^{(i)}\, \phi_\alpha(b^{(i)}) \right)$$
$$\times \prod_{i=n_\alpha}^{z-1} \left(\int_0^\infty \mathrm{d}\sigma^{(i)}\, g_\beta(\sigma^{(i)}) \int_0^\infty \mathrm{d}b^{(i)}\, \phi_\beta(b^{(i)}) \right) \delta\left(b - b_\alpha^{(0)}\right). \tag{A.3}$$

Since $\phi_\alpha(b)$ is actually a series of delta functions, it is convenient to introduce the Laplace transform of $\phi_\alpha(b)$, generally known as the moment-generating function

$$B_\alpha(q) \equiv \int_0^\infty \mathrm{e}^{-qb} \phi_\alpha(b)\,\mathrm{d}b. \tag{A.4}$$

In the present study, this quantity is named the branch-generating function. Equation (A.4) combined together with (4) leads to

$$\bar{b}_\alpha = -B_\alpha'(0), \tag{A.5}$$

which means the average branch conductivity is just the negative first derivative of $B_\alpha(q)$ evaluated at $q = 0$. Taking the Laplace transform of equation (A.3), it can be shown that

$$B_\alpha(q) = C_\alpha(q)^{n_\alpha - 1} C_\beta(q)^{n_\beta}, \tag{A.6}$$

where

$$C_\alpha(q) = \int_0^\infty \mathrm{d}\sigma\, g_\alpha(\sigma) \int_0^\infty \mathrm{d}b\, \phi_\alpha(b) \exp\left(-\frac{q\sigma b}{\sigma + b}\right). \tag{A.7}$$

Therefore, on account of (A.6), $C_\alpha(q)$ and $C_\beta(q)$ can be named the subbranch generating functions and, in analogy with (A.5), one can define the subbranch average conductivity as

$$\bar{b}_\alpha^{(i)} = -C'_\alpha(0). \tag{A.8}$$

Since $\phi_\alpha(b)$ and $g_\alpha(\sigma)$ are the probability densities normalized to unity, see (3) and (A.2), respectively, the boundary condition for $C_\alpha(q)$ at $q = 0$ is

$$C_\alpha(0) = 1. \tag{A.9}$$

The other boundary condition at $q = \infty$ is identified as the probability of having the finite cluster, R, since the main contribution to the integral (A.7) comes from the neighborhood of $b = 0$ or $\sigma = 0$:

$$C_\alpha(\infty) = R. \tag{A.10}$$

After some algebra [17] which involves an additional Laplace transform that introduces a new variable t, one obtains the integral equation

$$\int_0^\infty \mathrm{e}^{-tq} C_\alpha(q)\,\mathrm{d}q = \int_0^\infty \mathrm{d}\sigma\, g_\alpha(\sigma)(t+\sigma)^{-1} \times \left[1 + \frac{\sigma^2}{t+\sigma} \int_0^\infty \exp\left(-\frac{q\sigma t}{\sigma + t}\right) B_\alpha(q)\,\mathrm{d}q\right] \tag{A.11}$$

which is the final exact result to be solved asymptotically.

Appendix B. Near-mean-field expansion

Consider the integrals on both sides of equation (A.11). These integrals will be approximated for large t values using the Laplace method [38]. The method is based on the idea that the main contribution to the integrals comes from the neighborhood of $q = 0$, which makes it possible to use the Taylor series expansion as follows:

$$\begin{aligned} C_\alpha(q) &= \mathrm{e}^{\ln[C_\alpha(0) + qC'_\alpha(0) + \cdots]} \\ &= \mathrm{e}^{qC'_\alpha(0)}\left[1 + \sum_{l=2}^{\infty} a_\alpha^{(l)} q^l\right], \qquad \text{for} \qquad q \ll 1. \end{aligned} \tag{B.1}$$

This defined the coefficients $a_\alpha^{(l)}$. In addition, we have the $d_\alpha^{(l)}$ coefficients given by

$$C_\alpha(q)^m = \mathrm{e}^{mqC'_\alpha(0)} \sum_{l=0}^{\infty} d_\alpha^{(l)} q^l, \tag{B.2}$$

where $d_\alpha^{(0)} = 1$. Substituting (B.2) and its conjugate β analog into (A.6) and then using this in (A.11), one obtains

$$\int_0^\infty \mathrm{e}^{-tq} C_\alpha(q)\,\mathrm{d}q = \int_0^\infty \mathrm{d}u\, g_\alpha(u) \left\{\frac{1}{t - \tau_\alpha(u)} + \frac{u^2}{(t+u)^2} \sum_{k=2}^{\infty} d_\alpha^{(k)} \frac{k!}{s_\alpha^{k+1}}\right\}, \tag{B.3}$$

where

$$s_\alpha = \frac{ut}{u+t} - (n_\alpha - 1)C'_\alpha(0) - n_\beta C'_\beta(0), \tag{B.4}$$

$$\tau_\alpha(u) = \frac{u[(n_\alpha - 1)C'_\alpha(0) + n_\beta C'_\beta(0)]}{u - (n_\alpha - 1)C'_\alpha(0) - n_\beta C'_\beta(0)}. \tag{B.5}$$

Formula (B.3) represents an expansion in inverse powers of z which is seen from (B.4) and (B.5). Inversion of the Laplace transform in (B.3) yields

$$C_\alpha(q) = \int_0^\infty \mathrm{d}u\, g_\alpha(u) \exp[q\tau_\alpha(u)] \\ \times \left[1 + \sum_{k=2}^{\infty} d_\alpha^{(k)} k! \sum_{r=0}^{k-1} \frac{{}_{k-1}C_r}{(k-r)!} \frac{u^{2(k-r)} q^{k-r}}{[u - (n_\alpha - 1)C'_\alpha(0) - n_\beta C'_\beta(0)]^{2k-r}}\right],$$

where ${}_{k-1}C_r$ are the binomial coefficients. The equation right above is combined with (B.1), and then one equates term by term the factors of the successive powers of q and obtains

$$1 = \int_0^\infty \mathrm{d}u\, g_\alpha(u) \tag{B.6}$$

for $l = 0$ and

$$0 = \int_0^\infty \mathrm{d}u\, g_\alpha(u)[\tau_\alpha(u) - C'_\alpha(0)] + \sum_{m=2}^{\infty} d_\alpha^{(m)} I_\alpha^{(m10)} \tag{B.7}$$

$$a_\alpha^{(k)} = a_\alpha^{(k)0} + \sum_{m=2}^{\infty} d_\alpha^{(m)} \sum_{s=0}^{\min\{m-1,\,k-1\}} I_\alpha^{(mks)}, \qquad k \geqslant 2, \tag{B.8}$$

for $l = 1$, where

$$a_\alpha^{(k)0} = \int_0^\infty \mathrm{d}u\, g_\alpha(u) \frac{[\tau_\alpha(u) - C'_\alpha(0)]^k}{k!} \tag{B.9}$$

and

$$I_\alpha^{(mks)} = \frac{m!\,{}_{m-1}C_s}{(s+1)!\,[k-(s+1)]!} \int_0^\infty \mathrm{d}u\, g_\alpha(u) \frac{u^{2(s+1)}[\tau_\alpha(u) - C'_\alpha(0)]^{k-(s+1)}}{[u - (n_\alpha - 1)C'_\alpha(0) - n_\beta C'_\beta(0)]^{m+s+1}}. \tag{B.10}$$

The first term on the right-hand side of (B.7) is the representation of the mean-field limit $z \to \infty$,

$$0 = \int_0^\infty \mathrm{d}u\, g_\alpha(u)[\tau_\alpha(u) - \overline{C}'_\alpha(0)], \tag{B.11}$$

and the sum over m gives the corrections in inverse powers of z. Two equations, obtained by the interchange of α and β in (B.11), will be solved neglecting $n_\alpha = n$ as it is a constant negligibly small compared to $z - 1$. (Here, in order to keep up with the Stinchcome's results, we expand in powers of inverse $z - 1$ and not z, which is equivalent.) Solving (B.11) we get, as the first solution, the isotropic mean-field conductivity:

$$\overline{C}'_\alpha(0)_{\mathrm{iso}} = -\sigma_\alpha(p - p_c). \tag{B.12}$$

Additionally, we obtain

$$\overline{C}'_\alpha(0) = -\frac{\sigma_\alpha \sigma_\beta (p - p_c) p}{\sigma_\alpha p_c + \sigma_\beta (p - p_c)}, \tag{B.13}$$

which is the anisotropic solution of main interest for us.

We now move to some elaboration regarding the orders of correction contained in (B.7)–(B.10). One finds that $I_\alpha^{(210)} d_\alpha^{(2)}$ is of the order $(z-1)^{-2}$, since $I_\alpha^{(m10)}$ and $d_\alpha^{(m)}$ are of the orders $(z-1)^{-(m+1)}$ and $(z-1)^{m/2}$, respectively. Note that the correction to $a_\alpha^{(2)0}$ given by the first term of the sum in (B.8) affects $I_\alpha^{(210)} d_\alpha^{(2)}$ by the $(z-1)^{-4}$ order. Thus, to have the final result up to and including $\mathrm{O}([z-1]^{-4})$, the first term in the sum given by (B.8) should be taken into account, but only $a_\alpha^{(m)0}$ can be used for $m > 2$. In addition, when approximating $a_\alpha^{(m)}$ and $I_\alpha^{(m10)}$ with $m > 2$, we use the replacement $C'_\alpha(0) = \overline{C}'_\alpha(0)$. This is perfectly acceptable if $m > 2$, since any correction to this would be of $(z-1)^{-2}$ order, and hence would contribute to $a_\alpha^{(m)0}$ as $(z-1)^{-2m}$. To compute the error introduced by this substitution for $m = 2$, we expand $T_\alpha = I_\alpha^{(210)} a_\alpha^{(2)0}$ near $\bar{T}_\alpha = \overline{I}_\alpha^{(210)} \overline{a}_\alpha^{(2)0}$:

$$T_\alpha = \bar{T}_\alpha + (D^\alpha T_\alpha)\Delta C_\alpha + (D^\beta T_\alpha)\Delta C_\beta, \tag{B.14}$$

where $\Delta C_\alpha = C'_\alpha(0) - \overline{C}'_\alpha(0)$, $D^\beta T_\alpha = [\partial T_\alpha / \partial C'_\beta(0)]_{\overline{C}'_\beta(0)}$. Additionally, from (B.7) with the term $m = 2$ only, one has

$$-\bar{T}_\alpha = (D^\alpha A_\alpha)\Delta C_\alpha + (D^\beta A_\beta)\Delta C_\beta, \tag{B.15}$$

where $D^\beta A_\alpha = \left[\partial \int \mathrm{d}u\, g_\alpha(u)[\tau_\alpha - C'_\alpha(0)]/\partial C'_\beta(0)\right]_{\overline{C}'_\beta(0)}$. The computation of the coefficients yields

$$\begin{aligned} D^\alpha T_\alpha &= -1 + \mathrm{O}([z-1]^{-1}),\\ D^\beta T_\alpha &= 0,\\ D^\alpha A_\alpha &= 0,\\ D^\beta A_\alpha &= (z-1)\overline{I}_\alpha^{(310)} \overline{d}_\alpha^{(2)0}. \end{aligned} \tag{B.16}$$

Equations (B.14)–(B.16) combined together give

$$\begin{aligned} T_\alpha &= \bar{T}_\alpha \left(1 + (z-1)\overline{I}_\alpha^{(310)} \overline{d}_\alpha^{(2)0} \frac{\bar{T}_\beta}{\bar{T}_\alpha}\right)\\ &= \bar{T}_\alpha + \mathrm{O}([z-1]^{-4}). \end{aligned} \tag{B.17}$$

Substituting this into (B.7), one obtains the expression that contains all corrections up to the $(z-1)^{-4}$ order:

$$\begin{aligned} 0 = \int g_\alpha(u)[\tau_\alpha(u) - C'_\alpha(0)] + (z-1) a_\alpha^{(2)0} I_\alpha^{(210)} \\ \times \left\{1 + (z-1) I_\alpha^{(220)} + (z-1)^2 a_\alpha^{(2)0} I_\alpha^{(310)} \frac{I_\beta^{(210)}}{I_\alpha^{(210)}}\right\} \\ + I_\alpha^{(310)} d_\alpha^{(3)0} + I_\alpha^{(410)} d_\alpha^{(4)0} + I_\alpha^{(510)} d_\alpha^{(5)0} + I_\alpha^{(610)} d_\alpha^{(6)0}. \end{aligned} \tag{B.18}$$

Direct computation of equations (B.9) and (B.10) yields

$$\overline{a}_\alpha^{(m)0} = \frac{1}{m!}(-1)^m \overline{C}'_\alpha(0)^m (1-p)\left[1 + (-1)^m \left(\frac{1-p}{p}\right)^{m-1}\right], \tag{B.19}$$

$$\overline{I}_\alpha^{(m10)} = \frac{m![\overline{C}'_\alpha(0) + \sigma_\alpha p]^{m+1}}{\sigma_\alpha^{m-1} p^m} \tag{B.20}$$

$$\overline{I}_\alpha^{(220)} = \frac{2(1-p)\overline{C}'_\alpha(0)[\overline{C}'_\alpha(0) + \sigma_\alpha p]^3}{\sigma_\alpha p^2}. \tag{B.21}$$

Finally, substituting (B.19)–(B.21) into (B.18) and using (A.5), we get the anisotropic conductivity in the form of a series expansion in successive powers of the inverse coordination number:

$$\overline{b_{\alpha\,(\mathrm{I})}} = -\sigma_\alpha \left(-\frac{p\sigma_\beta \Delta}{\sigma_\alpha p_c + \sigma_\beta \Delta} + \frac{\Delta}{p} \sum_{n=2}^{\infty} G^{(n)} \right), \tag{B.22}$$

where

$$\begin{aligned}
G^{(2)} &= \frac{p_c^2}{p^2} \Delta s, \\
G^{(3)} &= \frac{p_c^3}{p^5} \Delta^2 s [p(2p-1) + 3\Delta s], \\
G^{(4)} &= \frac{p_c^4}{p^6} \Delta^2 s \Bigg[3s^2\Delta - 2sp + \Delta(1 - 3p + 3p^2) \\
&\quad + 10\Delta^2 s \left(\frac{2p-1}{p} \right) + 15\Delta^3 s^2 \frac{1}{p^2} \Bigg], \\
G^{(n)} &= \mathrm{O}\big(p_c^n\big), \\
\Delta &= p - p_c \qquad \text{and} \qquad s = 1 - p.
\end{aligned} \tag{B.23}$$

Expansion (B.23) coincides with the result of [17] except that factor 5 in front of $\Delta^2 s\left(\frac{2p-1}{p}\right)$ for $G_\alpha^{(4)}$ needs to be replaced by 10 according to us.

Appendix C. Investigation of critical indices

In this appendix, we investigate the critical exponents by means of an asymptotic analysis of the integral equation (A.11) for p approaching p_c from above introducing a small parameter

$$\epsilon = \frac{p - p_c}{p_c}. \tag{C.1}$$

On the one hand, it is known [24] that the percolation probability P, defined on the Bethe lattice as $P = 1 - R^z$, can be expanded near the percolation threshold in series:

$$P(\epsilon) = B\epsilon + C\epsilon^2 + \mathrm{O}(\epsilon^3),$$

where B and C are constants and hence

$$R = 1 - \delta^{(1)}\epsilon - \delta^{(2)}\epsilon^2 + \mathrm{O}(\epsilon^3). \tag{C.2}$$

Here,

$$\delta^{(1)} = 2/(z-2), \tag{C.3}$$

while the numerical value of $\delta^{(2)}$ has no significance for us, as shown in the analysis set forth below.

On the other hand, the anisotropic conductivity expansion in terms of ϵ has not been previously addressed. Motivated by the analysis of [17], we propose a trial solution to (A.11) of the form

$$C_\alpha(q) = R + \epsilon C_\alpha^{(1)}(q) + \epsilon^2 C_\alpha^{(2)}(q), \tag{C.4}$$

where $C_\alpha^{(1,2)}(q)$ are slowly varying functions of q described by the scaling relations

$$C_\alpha^{(1,2)}(q) = f_\alpha^{(1,2)}(c_\alpha \epsilon q), \tag{C.5}$$

with c_α being a constant to be determined later.

Now the variables $s = t/(c_\alpha\epsilon)$ and $y = c_\alpha\epsilon q$ are defined. Substituting (C.2) and (C.4) on the left-hand side of (A.11), multiplying both sides by t and expressing the integrals in terms of the new variables, one finds

$$\int_0^\infty \mathrm{e}^{-sy}[C_\alpha(y) - 1]\,\mathrm{d}y = p_c \frac{\sigma_\alpha(1+\epsilon)}{(\sigma_\alpha + c_\alpha\epsilon s)^2} \times \int_0^\infty \exp\left(-\frac{sy\sigma_\alpha}{\sigma_\alpha + c_\alpha\epsilon s}\right)\left\{C_\alpha^{n_\alpha-1}C_\beta^{n_\beta} - 1\right\}\mathrm{d}y, \tag{C.6}$$

where $C_\alpha(y)$ are given by (C.4) and (C.5). A set of equations is obtained equating the ϵ-expansion coefficients of the same order on the left- and right-hand side of the integral equation (C.6). Firstly, equating the terms linear in ϵ we obtain

$$f_\alpha^{(1)}(y) = p_c\left[(n_\alpha - 1)f_\alpha^{(1)}(y) + n_\beta f_\beta^{(1)}(y)\right]. \tag{C.7}$$

As a result, the first correction is isotropic:

$$f_\alpha^{(1)}(y) = f_\beta^{(1)}(y) \equiv f^{(1)}(y). \tag{C.8}$$

Secondly, equating the terms proportional to ϵ^2 and using (C.8) yields

$$\int_0^\infty \mathrm{e}^{-sy} f_\alpha^{(2)}(y)\,\mathrm{d}y = \int_0^\infty \mathrm{d}y\,\mathrm{e}^{-sy}\left\{\frac{1}{\delta^{(1)}}(f^{(1)} - \delta^{(1)})^2 + (f^{(1)} - \delta^{(1)}) \times \left[1 + \frac{c_\alpha}{\sigma_\alpha}(-2s + s^2y)\right] + p_c\left[(n_\alpha - 1)f_\alpha^{(2)} + n_\beta f_\beta^{(2)}\right]\right\}. \tag{C.9}$$

Isotropic solution. When substituting $c_\alpha = \sigma_\alpha$, we recover the isotropic solution $f_\alpha^{(2)} = f_\beta^{(2)} = f^{(2)}$ satisfying

$$\int_0^\infty \mathrm{e}^{-sy} f^{(2)}(y)\,\mathrm{d}y = \int_0^\infty \mathrm{d}y\,\mathrm{e}^{-sy}\left\{\frac{1}{\delta^{(1)}}(f^{(1)} - \delta^{(1)})^2 + (f^{(1)} - \delta^{(1)})[1 - 2s + s^2y] + p_c[(n_\alpha - 1)f^{(2)}(y) + n_\beta f^{(2)}(y)]\right\}$$

and

$$0 = \int_0^\infty \mathrm{d}y\,\mathrm{e}^{-sy}\left\{\frac{1}{\delta^{(1)}}(f^{(1)} - \delta^{(1)})^2 + (f^{(1)} - \delta^{(1)})[1 - 2s + s^2y]\right\}. \tag{C.10}$$

This gives a simple solution:

$$f^{(1)}(y)_{\text{iso}} = \delta^{(1)}\xi(y), \tag{C.11}$$

where ξ is determined by solving numerically the differential equation of the second order:

$$y\xi'' = \xi(1 - \xi), \qquad \xi(0) = 1, \qquad \xi(\infty) = 0, \tag{C.12}$$

which gives $\xi'(0) = -0.762$.

Anisotropic solution. Here, we try $c_\alpha \neq \sigma_\alpha$ in (C.9) to obtain another solution. To simplify (C.9), we combine it with (C.10), which yields

$$\int_0^\infty \mathrm{e}^{-sy} f_\alpha^{(2)}(y)\,\mathrm{d}y = \int_0^\infty \mathrm{e}^{-sy}\left\{(f^{(1)} - \delta^{(1)})\left[\frac{c_\alpha}{\sigma_\alpha} - 1\right](-2s + s^2y) + p_c\left[(n_\alpha - 1)f_\alpha^{(2)}(y) + n_\beta f_\beta^{(2)}(y)\right]\right\}\mathrm{d}y.$$

From this equation it follows that

$$f_\alpha^{(2)} - p_c\left[(n_\alpha - 1)f_\alpha^{(2)} + n_\beta f_\beta^{(2)}\right] = \frac{c_\alpha - \sigma_\alpha}{\sigma_\alpha}\delta^{(1)}x\xi''(x), \tag{C.13}$$

where x is an arbitrary variable. The quantities $f_\alpha^{(2)}(x)$ and $f_\beta^{(2)}(x)$ have to be symmetric with respect to the $\alpha \leftrightarrow \beta$ interchange. This condition is satisfied only in the following two cases:

$$n_\alpha \sigma_\beta = n_\beta \sigma_\alpha, \tag{C.14}$$

$$c_\alpha = \sigma_\beta, \tag{C.15}$$

or

$$n_\alpha = n_\beta, \tag{C.16}$$

$$c_\alpha = 2\sigma_\alpha\sigma_\beta/(\sigma_\alpha + \sigma_\beta). \tag{C.17}$$

The second set of conditions, equations (C.16) and (C.17), is inappropriate here due to the condition $z \gg n$ utilized in appendix B. Hence, from (C.14) we have

$$n_\alpha = z\sigma_\alpha/(\sigma_\alpha + \sigma_\beta), \qquad n_\beta = z - n_\alpha. \tag{C.18}$$

Substitution of (C.18) into (C.13) yields

$$f_\alpha^{(2)}(x) - f_\beta^{(2)}(x) = -\delta^{(1)} x \xi''(x) \frac{z-1}{z} \frac{\sigma_\alpha^2 - \sigma_\beta^2}{\sigma_\alpha \sigma_\beta}. \tag{C.19}$$

The latter is symmetric with respect to the reversal of α and β. Finally, combining (C.4), (C.5), (C.3), (C.11) and (C.15), we write the anisotropic solution:

$$C_\alpha(q) = R + \frac{2}{z-2}\xi(\sigma_\beta \epsilon q)\epsilon + f_\alpha^{(2)}(\sigma_\beta \epsilon q)\epsilon^2. \tag{C.20}$$

Then, using (A.5), (5) and (C.18), we obtain the average conductivity up to and including the ϵ^3 order:

$$\overline{\sigma_{\alpha\,(\mathrm{II})}} = \frac{z\sigma_\alpha}{\sigma_\alpha + \sigma_\beta}\left\{0.762\frac{2}{z-2}\sigma_\beta\epsilon^2 - \sigma_\beta f_\alpha^{(2)'}(q)\epsilon^3\right\} + C\epsilon^3, \tag{C.21}$$

where C is a constant which could be determined by equating the terms proportional to ϵ^3 in the expansion of equation (C.6). As a result, the first term in the expansion (C.21), proportional to ϵ^2, is the symmetric one. In addition, we can calculate the difference in the derivatives of $f_\alpha^{(2)}$ and $f_\beta^{(2)}$ using equations (C.19) and (C.12), which yields

$$\overline{\sigma_\alpha} - \overline{\sigma_\beta} = 0.762\frac{2(z-1)}{z-2}(\sigma_\alpha - \sigma_\beta)\epsilon^3. \tag{C.22}$$

Therefore, we have

$$\frac{\overline{\sigma_\alpha} - \overline{\sigma_\beta}}{\overline{\sigma_\beta}} = \frac{z-1}{z}\frac{\sigma_\alpha^2 - \sigma_\beta^2}{\sigma_\alpha\sigma_\beta}\epsilon. \tag{C.23}$$

References

[1] Broadbent S R and Hammersley J M 1957 *Proc. Camb. Phil. Soc.* **53** 629
[2] Kirkpatrick T R 1973 *Rev. Mod. Phys.* **45** 574
[3] Borcea L and Papanicolau G C 1998 *SIAM J. Appl. Math.* **58** 501
[4] Xu C, Hui P M and Li Z Y 2001 *J. Appl. Phys.* **90** 365
[5] Acharyya M and Chakrabarti B K 1995 *J. Phys. France I* **5** 153
[6] Turban L 1979 *J. Phys. C: Solid State Phys.* **12** 1479
[7] Blanc R, Mitescu C D and Thevenot G 1980 *J. Phys. France* **41** 387
[8] Friedman S P and Seaton N A 1998 *Transp. Por. Med.* **30** 241

[9] Redner S and Stanley H E 1979 *J. Phys. A: Math. Gen.* **12** 1267
Nakanishi H, Reynolds P J and Redner S 1981 *J. Phys. A: Math. Gen.* **14** 855
[10] Gavrilenko P and Gueguen Y 1989 *Terra Nova* **1** 63
[11] Balberg I and Binenbaum N 1983 *Phys. Rev.* B **28** 3799
[12] Bernasconi J 1974 *Phys. Rev.* B **9** 4575
[13] Straley J P 1977 *J. Phys. C: Solid State Phys.* **10** 3009
[14] Bahr K 1997 *Geophys. J. Int.* **130** 649
[15] Bahr K and Simpson F 2002 *Science* **295** 1270
[16] Turcotte D L and Newman W I 1996 *Proc. Natl Acad. Sci. USA* **93** 14295
[17] Stinchcombe R B 1974 *J. Phys. C: Solid State Phys.* **7** 179
[18] Straley J P 1980 *J. Phys. C: Solid State Phys.* **13** 4335
[19] de Gennes P G 1976 *J. Phys. Lett. France* **37** L1
[20] Sahimi M, Heiba A A, Hughes B D, Scriven L E and Davis H T 1982 *SPE Reservoir Eng.* **10969** 1
Heiba A A, Sahimi M, Scriven L E and Davis H J 1982 *SPE Reservoir Eng.* **11015** 123
[21] Sahimi M 1993 *Rev. Mod. Phys.* **65** 1393
[22] Sahimi M 2003 *Heterogeneous Materials I: Linear Transport and Optical Properties* (Berlin: Springer)
[23] Gujrati P D and Bowman D 1999 *J. Chem. Phys.* **111** 8151
[24] Stauffer D and Aharony A 2003 *Introduction to Percolation Theory* 2nd edn (London: Taylor and Francis)
[25] Skal A S and Shklovskii B I 1975 *Sov. Phys.—Semicond.* **8** 1029
[26] de Gennes P G 1976 *La Recherte* **7** 919
[27] Sarychev A K and Vinogradov A P 1983 *J. Phys. C: Solid State Phys.* **16** L1073
[28] Carmona F and Amarti A El 1987 *Phys. Rev.* B **35** 3284
[29] Gujrati P D 1995 *Phys. Rev. Lett.* **74** 1367
[30] Stauffer D 1979 *Phys. Rep.* **54** 1
[31] Renshaw C E 1999 Computationally efficient models for the growth of large fracture systems *Fracture of Rock* ed M H Aliabadi (Southampton: WIT)
[32] Sahimi M 1994 *Applications of Percolation Theory* (London: Taylor and Francis) chapters 5, 12 and references therein
[33] Toker D, Azulay D, Shimoni N, Balberg I and Millo O 2003 *Phys. Rev.* B **68** 041403
[34] Clerc J P, Podolsky V A and Sarychev A K 2000 *Eur. Phys. J.* B **15** 507
[35] Burda Z, Correlia J D and Krzywicki A 2001 *Phys. Rev.* E **64** 046118
[36] Bollobás B 1981 *Discrete Math.* **33** 1
[37] Hughes B D 1996 *Random Walks and Random Environments* vol 2 (Oxford: Clarendon)
[38] de Bruijin N G 1958 *Asymptotic Methods in Analysis* (Amsterdam: North Holland)
Bender C M and Orszag S A 1978 *Advanced Mathematical Methods for Scientists and Engineers* (New York: McGraw-Hill)